Comparative characteristics between calyculin A-induced and thimerosal-induced hyperactivation of cryopreserved bovine spermatozoa

Miyamoto, Natsuko
Ohya, Akihiro
Duritahala
Sakase, Mitsuhiro
Harayama, Hiroshi

(Citation)
Journal of Reproduction and Development,69(3):170-177

(Issue Date)
2023

(Resource Type)
journal article

(Version)
Version of Record

Journal of Reproduction and Development, Vol. 69, No 3, 2023

Original Article

Comparative characteristics between calyculin A-induced and thimerosal-induced hyperactivation of cryopreserved bovine spermatozoa

Natsuko MIYAMOTO[1)*], Akihiro OHYA[1)*], DURITAHALA[1)], Mitsuhiro SAKASE[2)] and Hiroshi HARAYAMA[1, 3)]

[1)]*Laboratory of Reproductive Biology, Division of Animal Science, Department of Bioresource Science, Graduate School of Agricultural Science, Kobe University, Hyogo 657-8501, Japan*
[2)]*Hokubu Agricultural Technology Institute, Hyogo Prefectural Technology Center for Agriculture, Forestry and Fisheries, Hyogo 669-5255, Japan*
[3)]*Biosignal Research Center, Kobe University, Hyogo 657-8501, Japan*

Abstract. This study aimed to characterize calyculin A (CL-A)-induced and thimerosal-induced hyperactivation of cryopreserved bovine spermatozoa. Hyperactivation was effectively induced by treating with 10 nM CL-A for 60 min in the presence of cyclic AMP analogs, extracellular Ca^{2+}, and albumin or with 12.5 μM thimerosal briefly in the absence of these capacitation-supporting factors. Majority of the spermatozoa exhibiting CL-A-induced hyperactivation were characterized by the 3-dimensional helical movement with head rotation, higher degree of flagellar curvature, and faster beating of the flagella than those exhibiting thimerosal-induced hyperactivation of the 2-dimensional planar movement without head rotation. The CL-A-induced hyperactivation was linked to the activation of cAMP/protein phosphorylation-dependent signaling cascades and to the decreased activity of glycogen synthase kinase-3α (GSK-3α). In contrast, the thimerosal-induced hyperactivation was suppressed by pretreatment with CL-A and cyclic AMP analogs in the absence of $CaCl_2$ to activate cAMP/protein phosphorylation-dependent signaling cascades. Additionally, the intracellular Ca^{2+} level in live sperm flagella was significantly higher in the CL-A-treated samples than in the thimerosal-treated samples. These results indicate that CL-A-induced hyperactivation of cryopreserved bovine spermatozoa is an extracellular Ca^{2+}-dependent type with the 3-dimensional helical movement, which can be regulated not only by the activation of cAMP/protein phosphorylation-dependent signaling cascades, leading to a large enhancement of the intracellular Ca^{2+} level, but also by the reduction in GSK-3α activity. Considering the different characteristics of thimerosal-induced hyperactivation, our results suggest that the diversity of sperm hyperactivation arises from different combinations of flagellar bending and head rotation.
Key words: Flagellar bending, Glycogen synthase kinase-3α, Hyperactivated sperm, Movement trajectory, Sperm rotation

(**J. Reprod. Dev. 69:** 170–177, 2023)

Ejaculated spermatozoa initiate progressive movement through the action of bicarbonate and fructose, which are secreted from the male accessory genital glands [1, 2]. In flagella, cytoplasmic Ca^{2+} levels are downregulated by Ca^{2+} clearance systems. Specifically, cytoplasmic Ca^{2+} is excluded to the extracellular space by plasma membrane Ca^{2+}-ATPases and sodium-calcium exchangers and is also transported into the redundant nuclear envelope (RNE) of the neck by sarcoplasmic reticulum calcium ATPases (SERCAs) [3]. Subsequently, the spermatozoa gradually undergo a variety of capacitation-associated changes in female reproductive tracts, such as the removal of decapacitation factors from plasma membrane and the high level of activation of cyclic adenosine 3′,5′-monophosphate (cAMP)/protein phosphorylation-dependent signaling cascades [2, 4–6]. Thereafter, they exhibit fertilization-indispensable hyperactivation of flagella in response to a rapid increase in cytoplasmic Ca^{2+} which is mediated by the influx of extracellular Ca^{2+} via the CatSper channel and other plasma membrane channels, as well as by the mobilization of RNE-stored Ca^{2+} via the inositol trisphosphate receptor (IP_3R). Hyperactivation can be induced *in vitro* in mouse and hamster epididymal spermatozoa by simple incubation in a capacitation-supporting medium containing bicarbonate, Ca^{2+}, and albumin [7–9]. However, such simple incubation is poorly effective in inducing hyperactivation in bovine ejaculated spermatozoa [10] because they have strong protein phosphatases that suppress the cAMP/protein phosphorylation-dependent signaling cascades, leading to increased cytoplasmic Ca^{2+} levels [11, 12]. Hyperactivation of bovine spermatozoa is often induced by chemical treatment with direct raisers of cytoplasmic Ca^{2+} (*e.g.*, thimerosal as an inducer of the mobilization of RNE-stored Ca^{2+} into the cytoplasm and caffeine as an inducer of influx of extracellular Ca^{2+} to the cytoplasm) [13]. Conversely, it was also possible to induce hyperactivation in bovine spermatozoa by treatment with the protein phosphatase inhibitor calyculin A (CL-A) in the presence of a cell-permeable/phosphodiesterase-resistant cAMP analog (Sp-5,6-Dichloro-cBIMPS, cBiMPS) and a cholesterol acceptor bovine serum albumin (BSA) to activate cAMP/protein phosphorylation-dependent signaling cascades, leading to increased cytoplasmic Ca^{2+} levels [11, 12, 14]. Interestingly, the percentage

Received: January 31, 2023
Accepted: March 30, 2023
Advanced Epub: April 18, 2023

Correspondence: H Harayama (e-mail: harayama@kobe-u.ac.jp)
* Miyamoto N and Ohya A have contributed equally to this work.

of spermatozoa exhibiting CL-A-induced hyperactivation varies widely among ejaculates [11, 15]. Thus, we believe that evaluating the sperm potential in exhibiting hyperactivation might be valid for examining flagellar functions in bovine capacitated spermatozoa. However, no data are available regarding the motion characteristics of CL-A-induced hyperactivation in bovine spermatozoa.

To accumulate information regarding the motion characteristics of CL-A-induced hyperactivation in bovine spermatozoa, we investigated changes in the motility regulator "glycogen synthase kinase-3α (GSK-3α) of bovine sperm flagella" [16–18] and motility parameters in the CL-A-treated spermatozoa in the presence of cBiMPS, $CaCl_2$, and BSA. Moreover, in comparative experiments, we observed the motility parameters of spermatozoa treated with thimerosal, which induces the mobilization of RNE-stored Ca^{2+} into the cytoplasm. The obtained results show the different characteristics of CL-A-induced and thimerosal-induced hyperactivation of bovine spermatozoa and suggest the need for the subtyping of bovine sperm hyperactivation.

Materials and Methods

Reagents and sperm samples

All the reagents were purchased from FUJIFILM Wako Pure Chemical Corporation (Osaka, Japan), unless specified otherwise.

Cryopreserved bovine semen (approximately 5.0×10^7 cells/ml) from fertile sires and fertile sire candidates (older than 1 year) were provided by the Hokubu Agricultural Technology Institute, Hyogo Prefectural Technology Center for Agriculture, Forestry and Fisheries (the Hokubu Institute) and used with the permission of the Hokubu Institute under the research project plan "Improvement of Fertility Assay for Japanese Black Bull Spermatozoa (2016–2022)." In each experiment, 3–6 straws of cryopreserved semen from 3–6 bulls (one straw from each bull) were used to reduce the influence of inter-bull differences on the experimental results. After thawing in warm water (38.5°C within 30 sec), the sperm samples were mixed and washed three times using centrifugation at 700 × *g* in phosphate-buffered saline (PBS) containing 0.1% polyvinyl alcohol (PVA, the average molecular weight; 30,000–70,000, Cat. # P8136; Sigma-Aldrich Co., St Louis, MO, USA) to remove seminal plasma and the extender.

Induction of flagellar hyperactivation

In the experiments to induce hyperactivation by treatment with a protein phosphatase inhibitor in the presence of the cAMP analog, extracellular Ca^{2+}, and albumin [12], the washed spermatozoa (the sperm concentration; 2.5×10^7 cells/ml) were incubated at 38.5°C and 100% air (in the water bath) for 60, 120, and 300 min in Hepes-buffered medium (pH 7.4) [modified Krebs-Ringer Hepes medium (mKRH) with $CaCl_2$ (3.42 mM), plus cBiMPS (100 µM, BML-CN120-0001, Enzo Life Sciences, Farmingade, NY, USA) and BSA (4 mg/ml, A9418, Sigma-Aldrich)] containing CL-A as an inhibitor of the protein phosphatase 1 and protein phosphatase 2A (1, 5, 10, 50, or 100 nM, C5552, Sigma-Aldrich) [12] using plastic tubes (volume size 1.5 ml, 1-7521-01, As One Corporation, Osaka, Japan). cBiMPS and CL-A were dissolved in 10% (v/v) dimethyl sulfoxide (DMSO) as 4 mM stock solution and 100% DMSO as 0.1 mM stock solution, respectively, and then added to the medium. Dimethyl sulfoxide was added to equalize the concentration of the solvent in all samples. Aliquots of the samples were used for subsequent experiments before and after incubation.

In the experiments to induce hyperactivation with thimerosal, the washed spermatozoa (the sperm concentration; 2.5×10^7 cells/ml) were suspended in a medium [mKRH plus PVA (0.1%), without $CaCl_2$] containing thimerosal (12.5, 25, and 50 µM, T5125, Sigma-Aldrich) in the presence or absence of ethylenediamine-N,N,N',N'-tetraacetic acid, trisodium salt, trihydrate (EDTA 3Na, 2.5 mM, N002, Dojindo Laboratories, Kumamoto, Japan). Because we preliminarily observed that adding BSA reduced the occurrence of thimerosal-induced hyperactivation (data not shown), this medium did not contain BSA. Thimerosal, EDTA 3Na, and PVA were dissolved in PBS as 2.5 mM stock solution, in Milli Q water as 250 mM stock solution, and in Milli Q water as 1% stock solution, respectively, and then added to the medium. Milli Q water and PBS were added to equalize the concentration of the solvent among all samples. Immediately after suspension of washed spermatozoa in the medium, aliquots of the samples were used for subsequent experiments. Additionally, in the experiments to examine the effects of the activation of cAMP/protein phosphorylation-dependent signaling cascades on the induction of hyperactivation with thimerosal, the washed spermatozoa (the sperm concentration; 2.5×10^7 cells/ml) were incubated at 38.5°C for 15 and 60 min in medium [mKRH plus cBiMPS (100 µM) and CL-A (10 nM), without $CaCl_2$], and then exposed to 12.5 µM thimerosal. Immediately after exposure to thimerosal, aliquots of the samples were used for sperm motility assays.

Sperm motility assay

Sperm motility assays were performed according to our previously reported method with minor modifications [15, 19]. In brief, an aliquot (sample volume: 10 µl) of the samples was usually placed in a chamber with a depth of 50 µm (Fujihira Industry, Tokyo, Japan) on a warmed stage (38.5°C) of an upright microscope (Olympus Corporation, Tokyo, Japan). Semen Analysis Slide with a depth of 10 µm (CV 1010-10^2, sample volume: 3 µl, CellVision Technologies, Heerhugowaard, Netherlands) and Leja Standard Counting Chamber with a depth of 20 µm (SC-20-01-02-B, sample volume: 5 µl, IMV Technologies, L'Aigle, France) were also used in the comparative experiments of three kinds of chambers with different depths. Microscopic videos of the sperm suspensions were captured using a CMOS camera (BU238M, Toshiba Teli, Tokyo, Japan) with × 40 objective lenses at a frame rate of 100 Hz and were recorded as non-compressed videos (FCR-1, TechnoScope, Saitama, Japan). The captured videos were converted into sequential frame images (JPEG images) using "Free Video to JPG Converter" software. The motility patterns were determined for approximately 100 spermatozoa in each sample using sequential images from each video, which were played frame-by-frame using PowerPoint 2013 (Microsoft, Redmond, WA, USA). Motile spermatozoa and hyperactivated spermatozoa were identified as those exhibiting any type of flagellar movement and exhibiting asymmetrical and large amplitude bending of the middle piece (at least the central and distal parts) and the principal piece, respectively.

To investigate the hyperactivated movement patterns, we classified hyperactivated spermatozoa into three types [a three-dimensional (3D) helical type with sperm head rotation, a two-dimensional (2D) planar type without sperm head rotation, and a sticking type (hyperactivated spermatozoa with heads sticking to the bottom of the chamber or to other spermatozoa)] (Fig. 1 and Supplementary Video 1). Using ImageJ software (National Institute of Health, Bethesda, MD, USA), we measured the flagellar curvature ratios in images of hyperactivated spermatozoa exhibiting maximal bending of the flagellum, as described previously [20]. The beating frequencies (number of flagellar beatings/sec) of hyperactivated spermatozoa were measured using sequential images from videos that were played frame-by-frame using PowerPoint 2013.

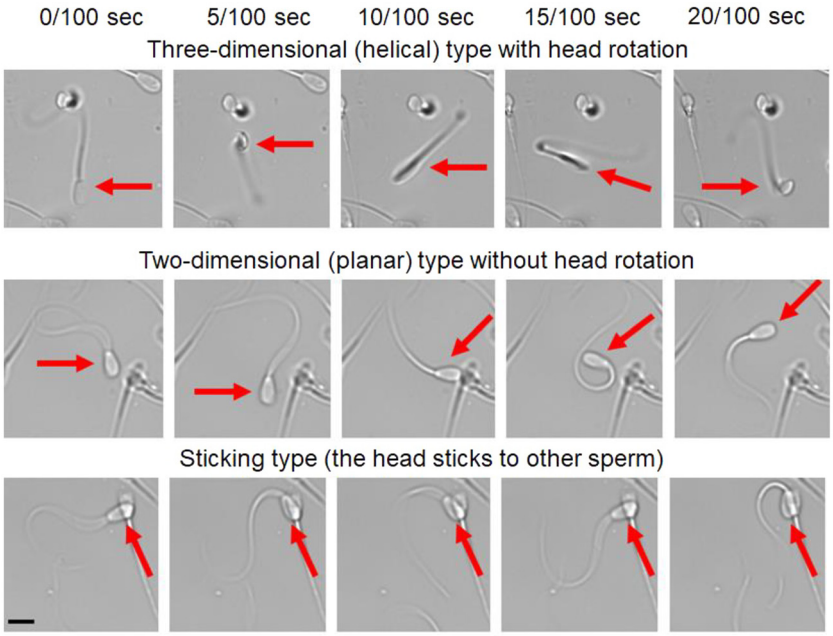

Fig. 1. Classification of hyperactivation of cryopreserved bovine spermatozoa. Microscopic images were collected every 5/100 sec from sequential images (frame rate 100 Hz) of videos of the three types of hyperactivated bovine spermatozoa. The scale bar indicates 10 µm. The red arrows indicate hyperactivated spermatozoa.

Observation of sperm movement trajectory

Sperm movement trajectories were recorded according to our previously reported method with minor modifications [21]. Briefly, after nuclear staining with SYBR14 (the final concentration: 120 nM, L7011, Thermo Fisher Scientific Inc., Waltham, MA, USA), a drop of sperm suspension (100 µl) was put on the pre-warmed silicon-coated glass slide (76 × 26 mm, S6111, Matsunami Glass Ind., Ltd., Kishiwada, Japan) and covered with the coverslip (50 × 24 mm, C024501, Matsunami) gently to make sufficient space for sperm 3D hyperactivation. The preparations of swimming spermatozoa were observed on a heated stage (38.5°C) of an upright microscope equipped with epifluorescence (U-FBW mirror unit composed of BP460-495 excitation filter, DM505 dichroic mirror, and BA510IF emission filter, Olympus), and sperm movement trajectories were captured using a CCD camera (DP73, Olympus) with the exposure time set to 2 sec.

Detection of cytoplasmic Ca^{2+} in sperm flagella

Cytoplasmic Ca^{2+} in sperm flagella was detected as described previously [22]. Briefly, the washed spermatozoa (1.0×10^8 cells/ml) were loaded with Fluo-3/AM (F023, Dojindo) in the presence of Pluronic F127 (0.02% v/v, R2443, Sigma-Aldrich) for 10 min in the dark and then washed. Fluo-3-loaded spermatozoa (2.5×10^7 spermatozoa/ml) were used to detect cytoplasmic Ca^{2+} after the abovementioned treatment to induce hyperactivation. For detection, the spermatozoa were mixed with propidium iodide (PI, L7011, Thermo Fisher Scientific, the final concentration: 12 µM) and used for observation under a microscope equipped with epifluorescence (U-FBW mirror unit). All images from each experiment were captured under the same conditions, and ImageJ software was used to measure the intensity of Fluo-3 fluorescence in the flagellum of each live (PI-negative) spermatozoon. The relative intensity of Fluo-3 fluorescence in the flagellum of each live spermatozoon was calculated using the following formula:

Relative Fluo-3 fluorescence intensity in the flagellum of each live spermatozoon (%)

= [(ImageJ value measured for each thimerosal (12.5 µM)-treated or CL-A (10 nM)-treated live spermatozoon) ÷ (average of the ImageJ values measured for thimerosal (12.5 µM)-treated live spermatozoa)] × 100

Western blotting and indirect immunofluorescence

Western blotting was performed using sperm extracts (2.4×10^6 cells/lane), polyvinylidene difluoride membrane (Merck Millipore Co., Darmstadt, Germany), Amersham ECL Prime Western Blotting Detection Reagent (RPN2232, GE Healthcare UK Limited, Buckinghamshire, UK), and AE-9300H Ez-Capture MG (ATTO Corporation, Tokyo, Japan) [19, 23]. The primary antibodies were rabbit anti-Ser/Thr-phosphorylated AGC kinase substrate polyclonal antibody (1:1000, Phospho-(Ser/Thr) PKA substrate antibody, #9621, Cell Signaling Technology, Inc., Beverly, MA, USA), rabbit anti-GSK-3α polyclonal antibody (1:250, 0.4 µg protein/ml, ab78664, Abcam, Cambridge, UK), and rabbit anti-Ser-phosphorylated GSK-3 polyclonal antibody (1:1000, 0.13 µg protein/ml, Anti-GSK-3β (phospho S9) + GSK-3α (phospho S21) polyclonal antibody, the antibody for detecting the inactive form, ab226877, Abcam). The secondary antibody was a horseradish peroxidase-conjugated donkey anti-rabbit immunoglobulin polyclonal antibody (1:5000 or 1:10000, NA934V, GE Healthcare).

Indirect immunofluorescence was performed as described previously [19, 24] using smear preparations of washed spermatozoa. The smear preparations were treated with 3% paraformaldehyde, 1% (v/v) Triton X-100 (X100-100ML, Sigma-Aldrich), rabbit anti-GSK-3α polyclonal antibody (1:50, 2.0 µg protein/ml), and Alexa Fluor 488-conjugated donkey anti-rabbit immunoglobulin polyclonal antibody (1:800, A21206, Life Technologies, Eugene, OR, USA).

Statistical analyses

Analyses of the data were performed using the *t*-test or one-way analysis of variance (ANOVA) after arcsine transformation (in cases the data did not include values above 1 [100%]) and tests for homogeneity of variance (Levene's test and Bartlett's test). Whenever the results of the F-test were significant in the ANOVA, individual averages were compared with one another using the Tukey-Kramer test. The level of significance was set at $P < 0.05$. Data of graphs are represented as averages + standard deviations. All data analyses were performed using Bell Curve for Excel (Version 3.21, Social Survey Research Information Co., Ltd., Tokyo, Japan), which was an add-in software for the Japanese version of Microsoft Excel 2016 (Microsoft).

Results

Optimal conditions of CL-A treatment to induce hyperactivation

To optimize CL-A treatment to induce hyperactivation in the presence of cBiMPS, $CaCl_2$, and BSA, the effects of CL-A concentrations (1–100 nM) and incubation periods on the motility and protein Ser/Thr phosphorylation states of the cryopreserved spermatozoa were examined. Although the percentages of motile spermatozoa tended to decrease with incubation time, irrespective of the CL-A concentration, the percentages of hyperactivated spermatozoa were significantly higher in the samples containing 10–100 nM and 5–100 nM CL-A after incubation for 60 and 120 min, respectively, compared to the control samples without CL-A (Fig. 2-A). In addition, treatment with 10 nM CL-A in medium without $CaCl_2$ did not induce hyperactivation (Supplementary Fig. 1).

Western blotting revealed that the addition of 10 nM CL-A to the medium increased the Ser/Thr-phosphorylated AGC kinase substrate proteins (31–58 kDa) in the samples incubated for 60 and 120 min, indicating that treatment with 10 nM CL-A for 60 or 120 min was effective in activating cAMP/protein phosphorylation-dependent signaling cascades (Fig. 2-B). Based on these results, treatment with 10 nM CL-A in the presence of cBiMPS, $CaCl_2$, and BSA for 60 min was used in the following experiments to induce hyperactivation.

Effects of CL-A treatment on motility regulator GSK-3α and motility patterns

Western blots of the extracts from washed spermatozoa (Supplementary Fig. 2) detected GSK-3α as an approximately 50 kDa band (the lower band). This molecular mass was the same as that determined using Western blotting of extracts from human somatic cells (see the data sheet from Abcam, https://www.abcam.co.jp/gsk3-alpha-antibody-ab78664.html). Moreover, GSK-3α was also detected as an approximately 55 kDa minor band (the upper band). Indirect immunofluorescence revealed that GSK-3α was localized in the flagellum (the middle and principal pieces) and head (the acrosome and postacrosomal region) of cryopreserved bovine spermatozoa (Supplementary Fig. 2). These observations agree with those of a previous report [16].

As shown in Western blots of Fig. 3, the 60-min treatment with 10 nM CL-A decreased the detection level of the lower band of GSK-3α, even though it had a slight effect on the detection of the upper band. In contrast, CL-A (10 nM) suppressed the decrease in the Ser21 phosphorylated (inactive) form of the upper band during the 60-min treatment, but it did not affect the decrease in the Ser21 phosphorylated (inactive) form of the lower band.

In the sperm samples after the 60-min treatment with 10 nM CL-A, majority of the hyperactivated spermatozoa were classified as a 3D helical type with head rotation on the chamber with a depth of 50 µm (Fig. 4 and Supplementary Video 2). The flagellar curvature ratios and beating frequencies were 0.25 ± 0.08 and 9.2 ± 1.3 beatings/sec, respectively (Fig. 5-B), and their movement trajectories were characterized by quadrangular and polygonal shapes (Fig. 5-C, trajectories iv-vi). However, when aliquots of the same samples were used for the sperm motility assay using different kinds of chambers with a depth of 10 or 20 µm, the percentages of hyperactivated spermatozoa significantly decreased (Fig. 4, Supplementary Fig. 3 and Supplementary Video 2).

Optimal conditions of thimerosal treatment to induce hyperactivation

To optimize thimerosal treatment to induce hyperactivation in the absence of cBiMPS and BSA, the effects of thimerosal (12.5–50 µM), $CaCl_2$ (1.71 mM), and EDTA 3Na (2.5 mM) on the motility of cryopreserved spermatozoa were examined. Exposure to thimerosal (12.5–50 µM) immediately induced hyperactivation in > 70% of motile spermatozoa, irrespective of the presence of $CaCl_2$ (1.71 mM) and EDTA 3Na (2.5 mM) (Fig. 5-A). In these sperm samples, > 70% of the hyperactivated spermatozoa exhibited 2D planar movement without head rotation and < 30% of them exhibited 3D helical movement with head rotation on the chamber with a depth of 50 µm (Fig. 5-B and Supplementary Video 2). However, thimerosal-induced hyperactivation could not be maintained for 10 min (data not shown). In the preliminary experiments, the addition of thimerosal (75–100 µM) immediately had deleterious influences on sperm motility and decreased the percentages of motile spermatozoa (data not shown). Based on these results, sperm samples that were briefly treated with 12.5 µM thimerosal in the absence of cBiMPS, $CaCl_2$, and BSA were used in the following experiments to induce hyperactivation.

Effects of brief treatment with thimerosal on motility characteristics

In the sperm samples treated briefly with 12.5 µM thimerosal, the flagellar curvature ratios (0.64 ± 0.11) and beating frequencies (6.6 ± 1.1 beatings/sec) were significantly different from those after the 60-min treatment with 10 nM CL-A (Fig. 5-B). In fact, there were large differences in sperm movement trajectories between these samples (Fig. 5-C). Specifically, the 3D hyperactivated spermatozoa of the CL-A-treated samples exhibited eight-figure movement and spiral movement, whereas the typical motion of the 2D hyperactivated spermatozoa of the thimerosal-treated samples was curvilinear or twisting (Fig. 5-C and Supplementary Video 1).

Effects of activation of cAMP/protein phosphorylation-dependent signaling cascades on thimerosal-induced hyperactivation

To activate sperm cAMP/protein phosphorylation-dependent signaling cascades in the absence of $CaCl_2$, sperm samples were supplemented solely with 100 µM cBiMPS or with 100 µM cBiMPS plus 10 nM CL-A and then exposed to 12.5 µM thimerosal before and after incubation for 15 and 60 min (Supplementary Fig. 4). Unexpectedly, supplementation with cBiMPS and CL-A strongly suppressed thimerosal-induced hyperactivation in the samples, irrespective of the incubation period (0, 15, and 60 min) but had no influence on the percentages of motile spermatozoa after thimerosal treatment. A similar suppression was observed in the samples containing cBiMPS before incubation (0 min), although the percentages of spermatozoa exhibiting thimerosal-induced hyperactivation after

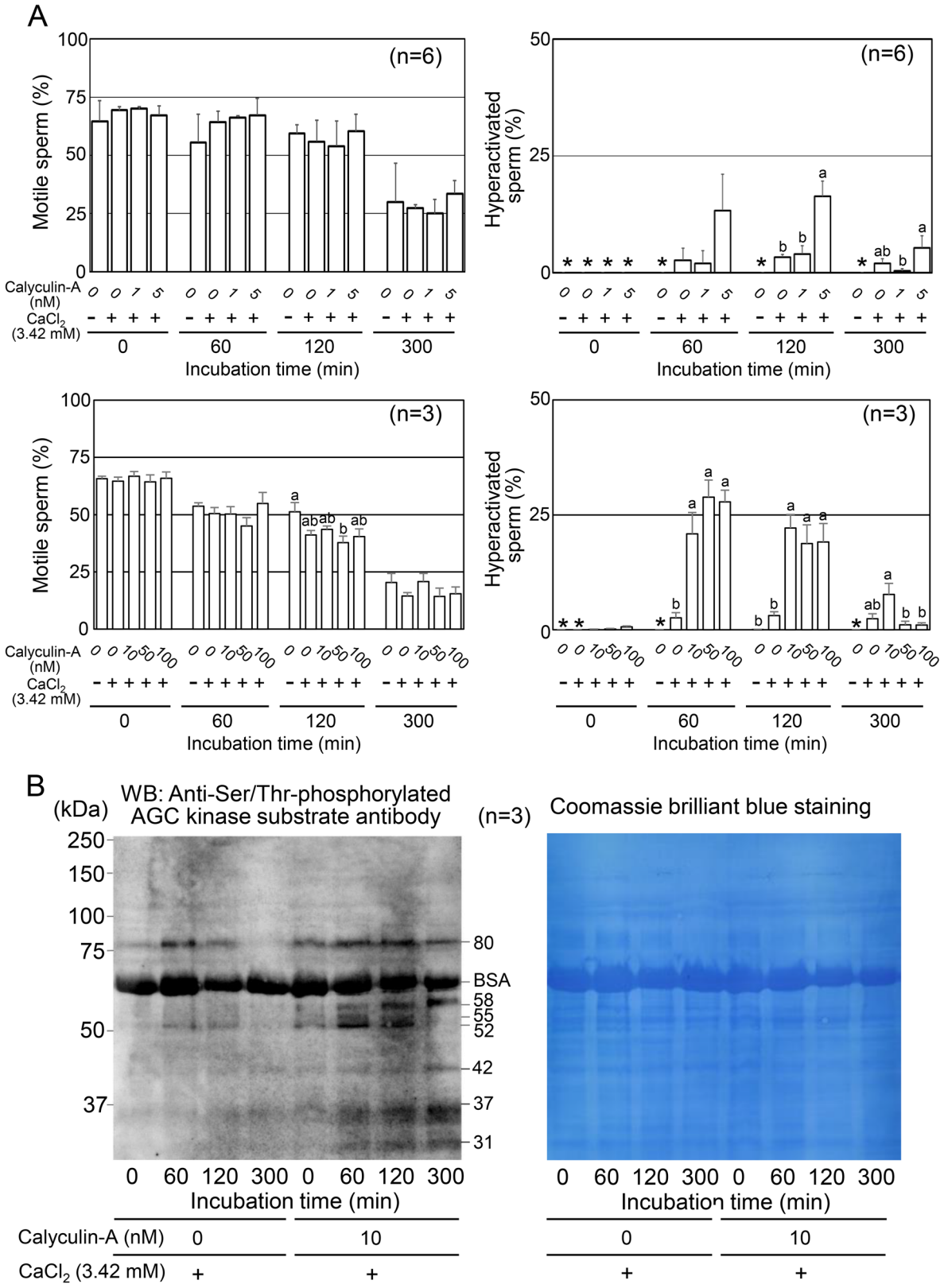

Fig. 2. Effects of calyculin A (CL-A), an inhibitor of protein phosphatases, on induction of hyperactivation in cryopreserved bovine spermatozoa. Washed spermatozoa were treated with CL-A (1–100 nM) in the presence of a cyclic AMP analog "Sp-5,6-Dichloro-cBIMPS" (cBiMPS, 100 μM) and a cholesterol acceptor "bovine serum albumin" (BSA, 4 mg/ml) for 60, 120, and 300 min. (A) Before and after treatment with 1–100 nM CL-A (the concentration ranges of the upper and lower figures were 1–5 nM and 10–100 nM, respectively), aliquots of the sperm samples were used for the motility assay using the chamber with a depth of 50 μm to determine percentages of motile spermatozoa and hyperactivated spermatozoa. Each bar of the graphs indicates mean + standard deviation (SD). Values with different letters (a, b) within the same groups are significantly different ($P < 0.05$). The bar with the asterisk was 0 ± 0% and excluded from statistical analyses. (B) Before and after treatment with 10 nM CL-A, aliquots of sperm samples were used for Western blotting with the anti-serine/threonine-phosphorylated AGC kinase substrate antibody, followed by Coomassie brilliant blue (CBB) staining. The results of CBB staining verified that the sperm samples were loaded equally on each lane of the gel.

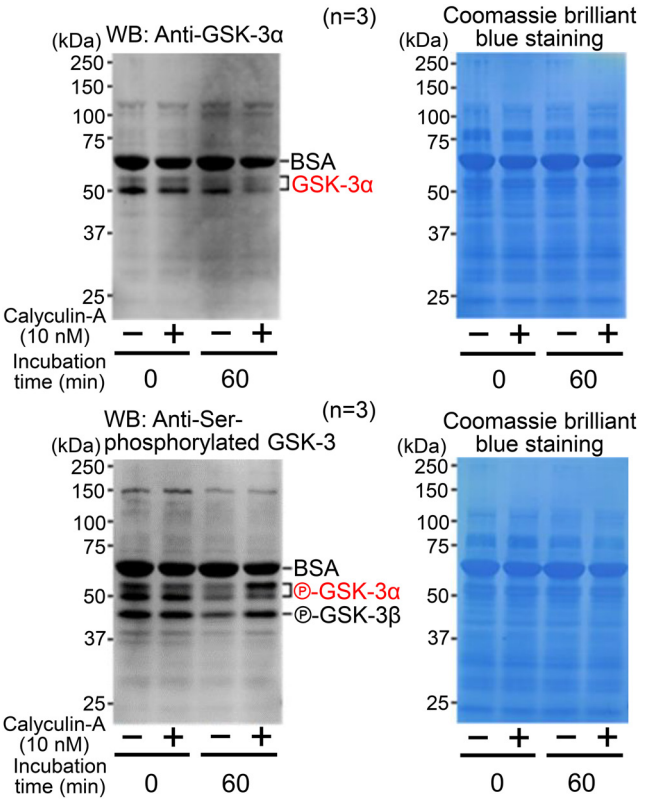

Fig. 3. Effects of treatment with CL-A on the amount and serine phosphorylation state of glycogen synthase kinase-3α (GSK-3α) in cryopreserved bovine spermatozoa. Washed spermatozoa were treated with CL-A (10 nM) in the presence of cBiMPS (100 μM) and BSA (4 mg/ml) for 60 min. Before and after treatment with 10 nM CL-A, aliquots of the sperm samples were used for Western blotting with the anti-GSK-3α antibody and anti-serine phosphorylated-GSK-3 (at serine 9 of GSK-3β and serine 21 of GSK-3α) antibody and subsequently for CBB staining. The results of CBB staining verified that the sperm samples were loaded equally on each lane of the gel.

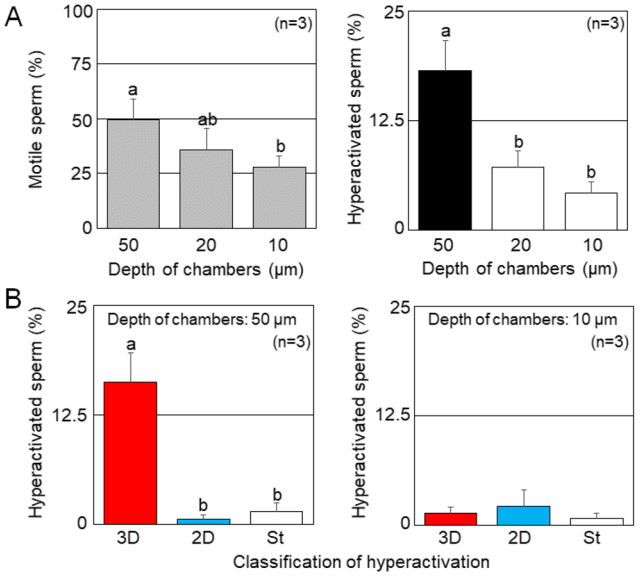

Fig. 4. Effects of different types of chambers on results of sperm motility assay. The washed spermatozoa were treated with CL-A (10 nM) in the presence of cBiMPS, $CaCl_2$, and BSA for 60 min. Aliquots of the same samples were placed in the chamber with a depth of 50, 20, and 10 μm on a warmed stage (38.5°C) of an upright microscope. The percentages of motile spermatozoa and hyperactivated spermatozoa were determined as described in Materials and Methods section. Hyperactivated spermatozoa are classified into the three-dimensional (3D) helical type with sperm head rotation, two-dimensional (2D) planar type without sperm head rotation, and sticking type (hyperactivated spermatozoa in which the heads stick to the chamber bottom or other spermatozoa) (St). Each bar of the graphs indicates mean + SD. Values with different letters (a, b) within the same groups are significantly different ($P < 0.05$). Please refer to additional data in Supplementary Fig. 3.

incubation for 15 and 60 min were almost equal between the control and cBiMPS-supplemented samples. Moreover, supplementation with cBiMPS alone slightly affected the induction of 3D helical hyperactivation with head rotation by exposure to thimerosal, and the flagellar curvature ratios and beating frequencies of spermatozoa exhibiting thimerosal-induced hyperactivation.

Intracellular Ca^{2+} levels in the flagella of live spermatozoa

The intensity of Fluo-3 fluorescence (cytoplasmic Ca^{2+} level) in the flagella of live (PI-negative) spermatozoa was compared between samples treated with CL-A for 60 min and those treated briefly with 12.5 μM thimerosal (Fig. 6). The former samples had large populations of live cells with more intensive Fluo-3 fluorescence in the flagella (ranging from 151–250%), and the average relative intensity of Fluo-3 fluorescence in the flagella of live spermatozoa was significantly higher in the former than in the latter.

Discussion

Sperm hyperactivation is characterized by the asymmetrization of flagellar bending with a large amplitude. This type of flagellar bending causes spermatozoa to exhibit circular and 2D planar movements. Moreover, the combination of extremely asymmetrical flagellar bending with steady rotation of the head yields hyperactivation with 3D helical movement [25], and both sperm behaviors are promoted by an increase in intracellular Ca^{2+} in cryopreserved bovine sperm flagella [22, 26]. In this study, Fig. 6 demonstrates that the intracellular Ca^{2+} level of cryopreserved bovine sperm flagella was significantly higher in samples treated with CL-A (10 nM) than in those treated with thimerosal (12.5 μM). Fig. 5-B depicts that the former samples contained much larger numbers of hyperactivated spermatozoa with 3D helical movement than the latter samples, and that the flagellar curvature ratio was much lower in the former. In addition, Supplementary Fig. 4 shows that treatment with thimerosal (12.5 μM) did not effectively induce hyperactivation with 3D helical movement in the samples that were pre-incubated in the absence of $CaCl_2$ to activate cAMP/protein phosphorylation-dependent signaling cascades. Altogether, these results suggest that a significant enhancement in the intracellular Ca^{2+} level in the flagella is necessary for the hyperactivation with 3D helical movement in cryopreserved bovine spermatozoa.

From the supplementary videos of previous reports [7, 27] and the present study (Supplementary Video 2), we can infer that hyperactivation with 3D helical movement in this study is equivalent to full-type hyperactivation of bovine spermatozoa and that thimerosal-induced hyperactivation of mouse epididymal spermatozoa is accompanied with 3D helical movement. In the present study, the induction of hyperactivation with 3D helical movement was dependent on the presence of extracellular Ca^{2+} in cryopreserved bovine spermatozoa

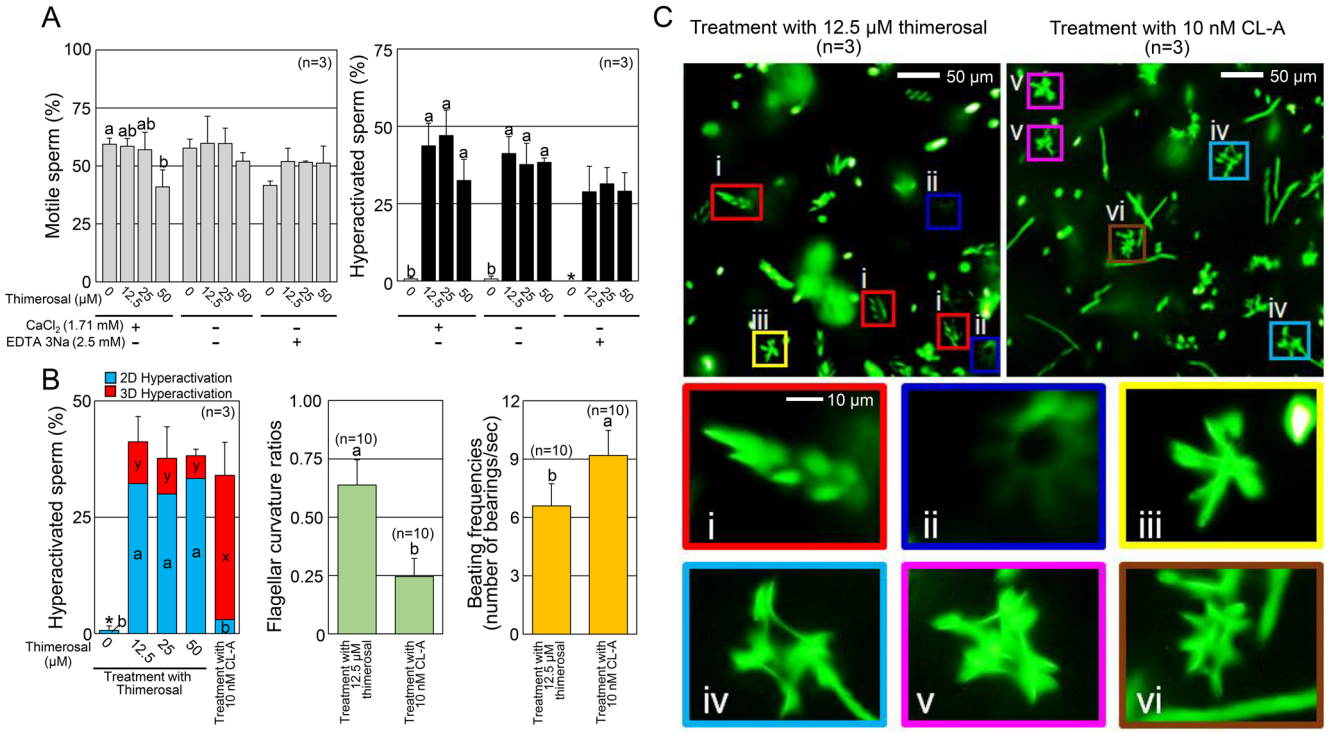

Fig. 5. Comparative characteristics of motility between CL-A-induced and thimerosal-induced hyperactivation of cryopreserved bovine spermatozoa. (A) Washed spermatozoa were briefly treated with thimerosal (12.5–50 μM) under the conditions indicated in the graphs. Aliquots of the sperm samples were used for motility assay using the chamber with a depth of 50 μm to determine percentages of motile spermatozoa and hyperactivated spermatozoa. (B) Characteristics of thimerosal-induced hyperactivation (in the absence of $CaCl_2$ and EDTA 3 Na, see above) and CL-A-induced hyperactivation (see the legends of Figs. 2 and 4) were compared. (A, B) Each bar of the graphs indicates mean + SD. Values with different letters (a, b and x, y) within the same groups are significantly different ($P < 0.05$). The bar with the asterisk was 0 ± 0% and excluded from statistical analyses. In the left graph of the panel B, SDs are for the total percentages of 2D and 3D hyperactivated spermatozoa. (C) Movement trajectories of SYBR14-stained spermatozoa which were treated shortly with 12.5 μM thimerosal in the absence of $CaCl_2$ and EDTA 3Na or with 10 nM CL-A in the presence of cBiMPS, $CaCl_2$, and BSA for 60 min were recorded under the fluorescent microscope for the exposure time of 2 sec.

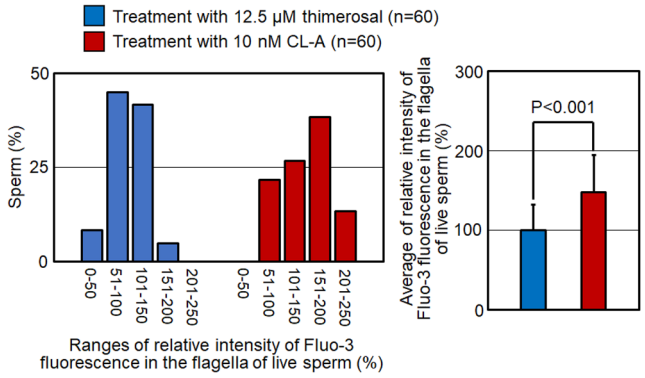

Fig. 6. Flagellar cytoplasmic Ca^{2+} levels of cryopreserved bovine spermatozoa after treatment for CL-A-induced and thimerosal-induced hyperactivation. Fluo-3-loaded spermatozoa were treated briefly with 12.5 μM thimerosal in the absence of $CaCl_2$ and EDTA 3Na or with 10 nM CL-A in the presence of cBiMPS, $CaCl_2$, and BSA for 60 min, mixed with propidium iodide (PI) and relative Fluo-3 fluorescence intensity in the flagellum of each live (PI-negative) spermatozoon was determined as described in the part of Materials and Methods.

(Supplementary Fig. 1). In contrast, the induction of hyperactivation with 3D helical movement (anti-hook type) in mouse epididymal spermatozoa was independent of extracellular Ca^{2+} and highly dependent on the thimerosal-induced mobilization of RNE-stored Ca^{2+} through IP_3R to the cytoplasm [7], whereas thimerosal treatment did not effectively induce hyperactivation with 3D helical movement in cryopreserved bovine spermatozoa (Fig. 5-B). Because cryopreserved bovine spermatozoa and mouse epididymal spermatozoa are mainly used to produce offspring using AI and *in vitro* fertilization, respectively, comparing these spermatozoa is important in the field of reproductive biotechnology. These results suggest that the origins from which adequate Ca^{2+} molecules are supplied to the flagellar cytoplasm to induce hyperactivation with 3D helical movement differ between cryopreserved bovine spermatozoa and mouse epididymal spermatozoa. Although further experiments are required to reveal the factors causing the difference in flagellar Ca^{2+} homeostasis between these spermatozoa, one of the causal factors may be explained by our previous observation that the cryopreservation process partially destroys SERCAs which increase the cumulative dosage of Ca^{2+} in the RNE internal store of the bovine sperm neck [22].

As reviewed by Dey *et al.* [17], the activities of GSK-3α and GSK-3β are modulated by CL-A-sensitive protein phosphatase 1 (PP1)-dependent dephosphorylation at Ser21 of the α isoform and at Ser9 of the β isoform. Mammalian spermatozoa develop the ability to move coincidental with changes of the phosphorylation state of GSK-3α and GSK-3β during their transit through epididymis. Interestingly, *Gsk3α*-null male mice and *Gsk3β*-null male mice are infertile and fertile, respectively. Thus, at least GSK-3α is an indispensable regulator of sperm motility and fertilization. As shown

in the previous reports [12, 16] and in this study (Supplementary Fig. 2), both CL-A-sensitive PP1 and GSK-3α are co-localized in the flagellar principal piece of bovine spermatozoa. In bovine sperm samples treated to induce hyperactivation with 3D helical movement (Fig. 3), CL-A (10 nM) suppressed the decrease in the Ser21 phosphorylated (inactive) form in the upper band of GSK-3α and reduced the detection level of the lower band of GSK-3α. These results suggest that CL-A treatment suppresses GSK-3α activity not only by inhibiting CL-A-sensitive PP1-mediated-dephosphorylation of the upper band (a reversible manner) but also by decreasing the amount of the lower band (an irreversible manner), and that the decreased activity of GSK-3α may be linked to the occurrence of hyperactivation with 3D helical movement in cryopreserved bovine spermatozoa. However, to elucidate the detailed mechanism of treatment to induce CL-A-induced hyperactivation with 3D helical movement, it is important to find molecules that are functional in the CL-A-dependent decrease of the amount in the lower band of GSK-3α.

Previous motility assay results for cryopreserved bovine spermatozoa have varied depending on the type of chambers used [28]. In this study, using cryopreserved bovine sperm samples (Fig. 4 and Supplementary Fig. 3), the percentage of motile spermatozoa and hyperactivated spermatozoa significantly decreased with the increase in chamber shallowness. This decrease in hyperactivated spermatozoa with 3D helical movement is likely owing to the insufficiency of the sperm-swimming space in chambers that are 10 or 20 µm deep. In addition, it may be difficult for these hyperactivated spermatozoa to enter a chamber that is 10 µm deep. Therefore, a deep chamber (50 µm) is suitable for evaluating bovine sperm 3D hyperactivation.

In conclusion, CL-A-induced hyperactivation of cryopreserved bovine spermatozoa is characterized by the extracellular Ca^{2+}-dependent type with 3D helical movement, which may be regulated not only by the activation of cAMP/protein phosphorylation-dependent signaling cascades, leading to a large enhancement of the intracellular Ca^{2+} level, but also by decreasing GSK-3α activity. Considering the different characteristics of thimerosal-induced hyperactivation, the results of this study indicate that the diversity of sperm hyperactivation arises from different combinations of flagellar bending and head rotation and suggest the need for subtyping of bovine sperm hyperactivation.

Conflict of interests: The authors declare no conflicts of interest.

Acknowledgement

This work was supported in part by Grants-in-Aid from the Japan Society for the Promotion of Science to H.H. (grant number 22K05951).

References

1. **Okamura N, Tajima Y, Soejima A, Masuda H, Sugita Y.** Sodium bicarbonate in seminal plasma stimulates the motility of mammalian spermatozoa through direct activation of adenylate cyclase. *J Biol Chem* 1985; **260**: 9699–9705. [Medline] [CrossRef]
2. **Harayama H.** Roles of intracellular cyclic AMP signal transduction in the capacitation and subsequent hyperactivation of mouse and boar spermatozoa. *J Reprod Dev* 2013; **59**: 421–430. [Medline] [CrossRef]
3. **Olson SD, Fauci LJ, Suarez SS.** Mathematical modeling of calcium signaling during sperm hyperactivation. *Mol Hum Reprod* 2011; **17**: 500–510. [Medline] [CrossRef]
4. **Cross NL.** Role of cholesterol in sperm capacitation. *Biol Reprod* 1998; **59**: 7–11. [Medline] [CrossRef]
5. **Harrison RA, Gadella BM.** Bicarbonate-induced membrane processing in sperm capacitation. *Theriogenology* 2005; **63**: 342–351. [Medline] [CrossRef]
6. **Visconti PE, Krapf D, de la Vega-Beltrán JL, Acevedo JJ, Darszon A.** Ion channels, phosphorylation and mammalian sperm capacitation. *Asian J Androl* 2011; **13**: 395–405. [Medline] [CrossRef]
7. **Chang H, Suarez SS.** Two distinct Ca^{2+} signaling pathways modulate sperm flagellar beating patterns in mice. *Biol Reprod* 2011; **85**: 296–305. [Medline] [CrossRef]
8. **Sakamoto C, Fujinoki M, Kitazawa M, Obayashi S.** Serotonergic signals enhanced hamster sperm hyperactivation. *J Reprod Dev* 2021; **67**: 241–250. [Medline] [CrossRef]
9. **Miyashita M, Fujinoki M.** Effects of aging and oviductal hormones on testes, epididymides, and sperm of hamster. *Reprod Med Biol* 2022; **21**: e12474. [Medline] [CrossRef]
10. **Marquez B, Suarez SS.** Different signaling pathways in bovine sperm regulate capacitation and hyperactivation. *Biol Reprod* 2004; **70**: 1626–1633. [Medline] [CrossRef]
11. **Mizuno Y, Isono A, Kojima A, Arai MM, Noda T, Sakase M, Fukushima M, Harayama H.** Distinct segment-specific functions of calyculin A-sensitive protein phosphatases in the regulation of cAMP-triggered events in ejaculated bull spermatozoa. *Mol Reprod Dev* 2015; **82**: 232–250. [Medline] [CrossRef]
12. **Arai Y, Sakase M, Fukushima M, Harayama H.** Identification of isoforms of calyculin A-sensitive protein phosphatases which suppress full-type hyperactivation in bull ejaculated spermatozoa. *Theriogenology* 2019; **129**: 46–53. [Medline] [CrossRef]
13. **Ho H-C, Suarez SS.** An inositol 1,4,5-trisphosphate receptor-gated intracellular Ca^{2+} store is involved in regulating sperm hyperactivated motility. *Biol Reprod* 2001; **65**: 1606–1615. [Medline] [CrossRef]
14. **Sai S, Harayama H.** Polyvinyl alcohol, but not bovine serum albumin, promotes the induction of full-type hyperactivation in boar cyclic AMP analog-treated spermatozoa. *Anim Sci J* 2022; **93**: e13777. [Medline] [CrossRef]
15. **Saha SR, Sakase M, Fukushima M, Harayama H.** Effects of digoxin on full-type hyperactivation in bovine ejaculated spermatozoa with relatively lower survivability for incubation with stimulators of cAMP signaling cascades. *Theriogenology* 2020; **154**: 100–109. [Medline] [CrossRef]
16. **Vijayaraghavan S, Mohan J, Gray H, Khatra B, Carr DW.** A role for phosphorylation of glycogen synthase kinase-3alpha in bovine sperm motility regulation. *Biol Reprod* 2000; **62**: 1647–1654. [Medline] [CrossRef]
17. **Dey S, Brothag C, Vijayaraghavan S.** Signaling enzymes required for sperm maturation and fertilization in mammals. *Front Cell Dev Biol* 2019; **7**: 341. [Medline] [CrossRef]
18. **Ferreira AF, Santiago J, Silva JV, Oliveira PF, Fardilha M.** PP1, PP2A and PP2B interplay in the regulation of sperm motility: lessons from protein phosphatase inhibitors. *Int J Mol Sci* 2022; **23**: 15235. [Medline] [CrossRef]
19. **Wada A, Harayama H.** Calmodulin is involved in the occurrence of extracellular Ca^{2+}-dependent full-type hyperactivation in boar ejaculated spermatozoa incubated with cyclic AMP analogs. *Anim Sci J* 2021; **92**: e13552. [Medline] [CrossRef]
20. **Schmidt H, Kamp G.** Induced hyperactivity in boar spermatozoa and its evaluation by computer-assisted sperm analysis. *Reproduction* 2004; **128**: 171–179. [Medline] [CrossRef]
21. **Yamada A, Sakase M, Fukushima M, Harayama H.** Reconsideration of the evaluation criteria for bull ejaculated sperm motility in the context of rotation. *J Reprod Dev* 2018; **64**: 377–384. [Medline] [CrossRef]
22. **Duritahala SM, Sakase M, Harayama H.** Involvement of Ca^{2+}-ATPase in suppressing the appearance of bovine helically motile spermatozoa with intense force prior to cryopreservation. *J Reprod Dev* 2022; **68**: 181–189. [Medline] [CrossRef]
23. **Harayama H, Miyake M.** A cyclic adenosine 3′,5′-monophosphate-dependent protein kinase C activation is involved in the hyperactivation of boar spermatozoa. *Mol Reprod Dev* 2006; **73**: 1169–1178. [Medline] [CrossRef]
24. **Kojima A, Matsushita Y, Ogura Y, Ishikawa S, Noda T, Murase T, Harayama H.** Roles of extracellular Ca^{2+} in the occurrence of full-type hyperactivation in boar ejaculated spermatozoa pre-incubated to induce the cAMP-triggered events. *Andrology* 2015; **3**: 321–331. [Medline] [CrossRef]
25. **Suarez SS.** Control of hyperactivation in sperm. *Hum Reprod Update* 2008; **14**: 647–657. [Medline] [CrossRef]
26. **Ho HC, Granish KA, Suarez SS.** Hyperactivated motility of bull sperm is triggered at the axoneme by Ca^{2+} and not cAMP. *Dev Biol* 2002; **250**: 208–217. [Medline] [CrossRef]
27. **Harayama H.** Flagellar hyperactivation of bull and boar spermatozoa. *Reprod Med Biol* 2018; **17**: 442–448. [Medline] [CrossRef]
28. **Gloria A, Carluccio A, Contri A, Wegher L, Valorz C, Robbe D.** The effect of the chamber on kinetic results in cryopreserved bull spermatozoa. *Andrology* 2013; **1**: 879–885. [Medline] [CrossRef]